

Spin and charge ordering in three-leg ladders in oxyborates.

E. Vallejo and M. Avignon¹

¹*Laboratoire d'Etudes des Propriétés Electroniques des Solides (LEPES)-Centre National de la Recherche Scientifique (CNRS), BP 166, F-38042 Grenoble Cedex 9, France.*

(Dated: February 28, 2018)

We study the spin ordering within the 3-leg ladders present in the oxyborate $\text{Fe}_3\text{O}_2\text{BO}_3$ consisting of localized classical spins interacting with conduction electrons (one electron per rung). We also consider the competition with antiferromagnetic superexchange interactions to determine the magnetic phase diagram. Beside a ferromagnetic phase we find (i) a phase with ferromagnetic rungs ordered antiferromagnetically (ii) a zig-zag canted spin ordering along the legs. We also determine the induced charge ordering within the different phases and the interplay with lattice instability. Our model is discussed in connection with the lattice dimerization transition observed in this system, emphasizing on the role of the magnetic structure.

PACS numbers: 75.10.Hk; 71.45.Lr

The ordering of the local spins interacting with conduction electrons remains an important problem and has become very active in the context of manganites. The coupling can be antiferromagnetic as in heavy-fermions systems or Kondo insulators or ferromagnetic as a result of Hund's coupling in manganites. This gives rise to the general double exchange (DE) interactions¹ favoring a ferromagnetic background of local spins. This ferromagnetic tendency is expected to be thwarted by antiferromagnetic superexchange (SE) interactions between the localized spins leading to interesting and unusual magnetic states. Instead of the canted states conjectured by de Gennes², spin ordering consisting of ferromagnetic *islands* coupled antiferromagnetically has been identified for various commensurate fillings both for $S = 1/2$ quantum spins in one dimension³ and classical spins in two dimensions⁴. Carriers are found to be localized in the ferromagnetic islands giving rise to bond ordering and as a consequence leads to charge ordering.

The ludwigite oxy-borate system $\text{Fe}_3\text{O}_2\text{BO}_3$ may provide evidence of this mechanism for the existence of simultaneous spin and charge ordering resulting from the competition between DE and SE. Fe-ludwigite contains subunits in the form of 3-leg ladders (3LL) of Fe cations and presents an interesting structural and charge ordering transition at $T_c \approx 283\text{K}$, such that long and short bonds on the rungs alternate along the ladder axis⁵. As evidenced by Mössbauer studies^{6,7} and X-ray diffraction⁸ each rung can be viewed as three Fe^{3+} ions (*triad*) with high-spin $S = 5/2$ local spins sharing an extra itinerant electron. The charge distribution among the triads is a key issue. Spin ladders have recently attracted a considerable interest but we have here an interesting case of a spin ladder coupled with conduction electrons. The coupling is similar to the one encountered in Fe double-perovskite systems⁹. In the $\text{Fe}^{3+} d^5$ configuration all orbitals being occupied in one spin channel, itinerant electrons can hop to a site i only if its spin is antiparallel to the local spin \vec{S}_i . This is indeed equivalent to DE with an effective antiferromagnetic and *infinite exchange integral*. Antiferromagnetic SE interactions resulting from virtual

hopping among the $\text{Fe}-d^5$ configurations have been estimated, leading to strongly interacting spin units of the Fe-triads in which all nearest-neighbor (n.n) spins are antiferromagnetically coupled both above and below the structural transition temperature¹⁰ in contradiction with recent neutron results⁸. In addition, it can be shown that an homogeneous magnetic phase is not compatible with the observed charge distribution on the different Fe sites. In this letter we will show that the inclusion of the interaction between itinerant electrons and local spins will drastically improve this picture.

Since the local spins \vec{S}_i are fairly large $S = 5/2$ we will treat them as classical spins specified by their polar angles θ_i and φ_i ($0 < \theta_i < \pi$, $0 < \varphi_i < 2\pi$) defined as usual with respect to a z -axis taken as the spin quantization axis of itinerant electrons. Rotating the itinerant electron quantization axis on each site to make it parallel to \vec{S}_i , one gets the rotated electron operators with spin opposite to the local spin c_i^+ (c_i) in terms of the original electron operators $d_{i\sigma}^+$ ($d_{i\sigma}$) as $c_i^+ = \cos(\theta_i/2)d_{i\downarrow}^+ - e^{-i\varphi_i} \sin(\theta_i/2)d_{i\uparrow}^+$. The rotated electrons are indeed *spinless* electrons. The effective hopping between these electrons antiparallel to local spins at sites i and j is therefore given by $t_{i,j}^e = t_\nu(\cos \frac{\theta_i}{2} \cos \frac{\theta_j}{2} + e^{-i(\varphi_i - \varphi_j)} \sin \frac{\theta_i}{2} \sin \frac{\theta_j}{2})$, $t_\nu = t_a, t_c$ being the nearest neighbor (n.n) hopping integrals on the rungs and along the axis of the ladder.

So, to describe the magnetic structure, we represent the interaction between the Fe^{3+} localized spins \vec{S}_i and the itinerant electrons by the tight-binding Hamiltonian together with SE interactions among the local spins

$$H = - \sum_{\langle ij \rangle} (t_{i,j}^e c_i^+ c_j + h.c.) + \sum_{\langle ij \rangle} J_{ij} \vec{S}_i \cdot \vec{S}_j$$

$\langle ij \rangle$ represents n.n sites. We further assume that this band is non-degenerate, therefore the band filling is $n = 1/3$. We take the simple situation in which all the spins are in the same plane. This simplification is inspired by Monte Carlo simulations on 2D systems in which non-coplanar spin configurations never seem to appear⁴ and

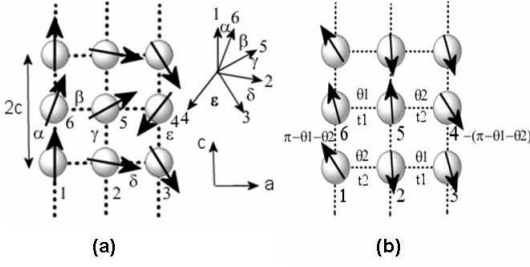


FIG. 1: (a) Magnetic structure of the 3-leg ladder Ludwigite. The five angles $\alpha, \beta, \gamma, \delta, \epsilon$ gives the orientation of the spins on the six sites $i = 1 - 6$ unit cell. (b) Magnetic structure of the I_a phase. This structure can present a zigzag modulation of the angles θ_1 and θ_2 .

is consistent with neutron scattering results⁸. All coplanar phases being degenerate, we choose the plane of the ladder, taking $\theta_i = \pi/2$ and the hopping terms simply becomes $t_{i,j}^e = \frac{t_a}{2}(1 + e^{-i(\varphi_i - \varphi_j)})$. Guided by the periodicity $2c$ of the low temperature distorted phase⁵, we consider a unit-cell containing two rungs. We define the magnetic structure by the five angles $\alpha, \beta, \gamma, \delta, \epsilon$ giving the orientation of the spins on the six sites $i = 1 - 6$ unit cell as shown in Fig. 1-a. $J_{ij} = J_a, J_c$ are SE interactions in the two directions.

The kinetic energy term favors a ferromagnetic arrangement of the local spins which competes with the SE, leading to a variety of complex structures. After the Fourier transformation, the dispersion of the conduction electrons is obtained from the tight-binding matrix with the wave-vector k in the c -direction, $-\pi/2c < k < \pi/2c$. In the general case, it consists of six bands $\epsilon_{i=1-6}(k)$, the values $\epsilon_i(k)$ are increasing from $i = 1$ to 6. For the band-filling $n = 1/3$ the two lowest bands $\epsilon_{1,2}$ only are occupied. We minimize the total energy with respect to the five angles $\{\alpha, \beta, \gamma, \delta, \epsilon\}$. Fig. 2 shows the phase diagram as function of $J_a S^2/t_c$ and $J_c S^2/t_c$ for a typical value $t = \frac{t_a}{t_c} = 1.2$ roughly estimated from the different Fe-Fe distances in the triad and along the legs. Besides the fully ferromagnetic (F) state characterized by the uniform angles $\alpha = \beta = \gamma = \delta = \epsilon = 0$, when J_a and J_c are not too large $J_c S^2/t_c \lesssim 0.07$ and $J_a S^2/t_c \lesssim 0.13$, we find two other phases (i) at larger J_c a phase A which is antiferromagnetic in the c -direction ($\alpha = \gamma = \epsilon = \pi$) with two different angles in the rung (ii) a phase I with different angles ($\alpha, \beta, \gamma, \delta, \epsilon$) which is the stable one in a large part of the phase diagram for lower J_c . These phases are further described below. Except for the ferromagnetic phase, there is a gap between the two lowest bands and the middle ones. At 1/3-filling the Fermi energy is located in this gap so that all these phases are

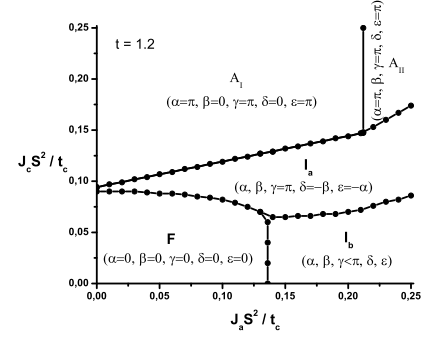


FIG. 2: Phase diagram as function of $\frac{J_a S^2}{t_c}$ and $\frac{J_c S^2}{t_c}$, for a typical value of $t = \frac{t_a}{t_c} = 1.2$. The different phases are described in the text.

insulating. For symmetry reason the same occurs also at 2/3-filling. This gap depends on the values of the different angles and can be direct or indirect.

In phase A the hopping is totally suppressed in the c -direction and the dispersion reduces to three energy levels. The particular phase A_I with fully ferromagnetic rungs ($\beta = \delta = 0$) is encountered at lower J_a . This phase is in qualitative agreement with the magnetic structure recently proposed from neutron experiments at 82K⁸. It is indeed very similar to a phase already found with Monte-Carlo calculations in the 2D model⁴. At larger J_a , canting occurs within the rungs with two different angles β, δ , we call this phase A_{II} .

Phase I presents very interesting simple structures as, for example, the phase I_a ($\alpha, \beta, \gamma = \pi, \delta = -\beta, \epsilon = -\alpha$) which can be defined in terms of only two angles θ_1 and θ_2 ($\beta = \theta_1, \alpha = \pi - \theta_1 - \theta_2$). It is AF along the central leg so that no hopping is taking place along this leg. This structure presents a zig-zag modulation of the angles θ_1 and θ_2 and, consequently of the hopping t_1, t_2 as shown in Fig. 1-b. A phase called I_b tends to a ferromagnetic behavior along c -direction with $\gamma < \pi$.

As soon as the central leg is AF ($\gamma = \pi$) the bands are two-fold degenerate with gaps at $k = \pm \frac{\pi}{2c}$. The dispersion of the bands are $\epsilon(k) = 0$ and

$$\epsilon(k) = \pm \left[1 + t^2 + \frac{1}{2} t^2 (\cos \theta_1 + \cos \theta_2) - \cos(\theta_1 + \theta_2) + (1 - \cos(\theta_1 + \theta_2)) \cos 2kc \right]^{\frac{1}{2}}.$$

The lower band is filled, precisely for $n = 1/3$, lowering the kinetic energy to stabilize this phase. The total energy per rung E can be expressed as

$$\begin{aligned} \frac{E}{t_c} = & -\frac{2}{\pi} \left[2 + t^2 + \frac{1}{2} t^2 (\cos \theta_1 + \cos \theta_2) + \right. \\ & \left. - 2 \cos(\theta_1 + \theta_2) \right]^{\frac{1}{2}} \mathcal{E}(q) - 2J_c \frac{S^2}{t_c} \left[\frac{1}{2} + \cos(\theta_1 + \theta_2) \right] \\ & + \frac{J_a S^2}{t_c} (\cos \theta_1 + \cos \theta_2), \end{aligned}$$

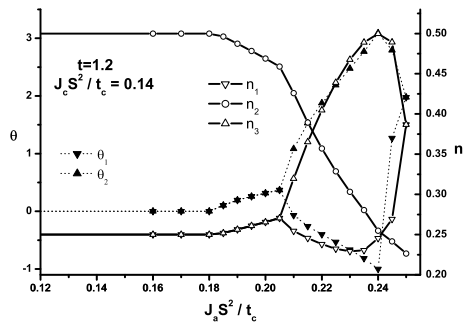


FIG. 3: Cut of the phase diagram along the line $\frac{J_c S^2}{t_c} = 0.14$, showing the angles between the spins and the resulting charges.

$\mathcal{E}(q)$ being the complete Elliptic Integral of second kind with parameter $q = \frac{2(1 - \cos(\theta_1 + \theta_2))}{2 + t^2 + \frac{1}{2}t^2(\cos\theta_1 + \cos\theta_2) - 2\cos(\theta_1 + \theta_2)}$.

The angle γ varies discontinuously between phase I_a ($\gamma = \pi$) and phases F ($\gamma = 0$) and I_b ($\gamma < \pi$), so these transitions are first order. All other transitions are second order. In the I_b phase, close to F we find a canted ferromagnetic phase with canting within the rungs, one angle only β (or equivalently δ) being different from zero; at the transition $\beta \rightarrow 0$ giving the second order boundary line $\frac{J_a S^2}{t_c} = \frac{t \arccos(-t/2\sqrt{2})}{4\pi\sqrt{2}}$. Between F and A_I phases, the I_a phase has essentially $\theta_1 = \theta_2 = \theta$; this can be seen for example, close to A_I , in Fig. 3 for $\frac{J_c S^2}{t_c} = 0.14$. Therefore the transition line between I_a and A_I ($\theta_1, \theta_2 \rightarrow 0$) is also second order corresponding to $\frac{J_c S^2}{t_c} = \frac{\sqrt{2}(4-t^2)}{32t} + \frac{J_a S^2}{4t_c}$. For larger values of $\frac{J_a S^2}{t_c}$ the phase evolves towards the more general zig-zag structure $\theta_1 \neq \theta_2$ (see Fig. 3).

As we mentioned the charge distribution is crucial in the Fe-ludwigite ladder so let us examine this point in detail. It is clear that bond ordering is linked to the spin ordering through the modulation of the hopping amplitudes. The ferromagnetic bonds tend to localize the extra electron. This in turn may induce different types of charge ordering on the non-equivalent Fe-sites in the rung. Experimentally^{6,7} two charge regimes are identified (i) above T_c , the side sites 1 and 3 are identical $n_1 = n_3 \sim 0.25 - 0.3$ while the central site 2 has more electrons $n_2 \sim 0.5$ (ii) below T_c down to 74K the charge on site 3 (the site which gets closer to site 2) increases close to the charge of site 2 which remains stable, $n_2 \approx n_3 \sim 0.5$, and at the same time the charge of site 1 decreases to $n_1 \sim 0.15$. Of course these values⁸ indicate only the tendencies, since one should have $n_1 + n_2 + n_3 = 1$. However below 74K two contradictory behaviours have been reported^{7,11}. Douvalis et al¹¹ found that the low temperature ordering below T_c persists down to $T = 0$, while Larrea et al⁷ recover the same charge ordering as above T_c .

To begin with, let us look at homogeneous magnetic phases i.e a phases without modulation of the hopping

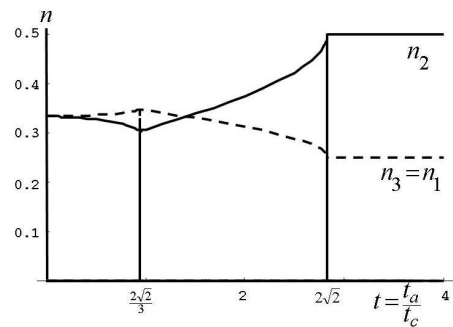


FIG. 4: Electronic distribution n_i of the homogeneous magnetic phase as function of t .

amplitude; in this sense ferromagnetic and paramagnetic phases are equivalent, only the effective hoppings are different in the two cases. The electronic distribution is shown in Fig. 4 as a function of t . We see that the high temperature behaviour can be reproduced only if t is large $t \gtrsim 2.5 - 3$, in particular for $t \geq 2\sqrt{2}$ one gets $n_1 = n_3 = 1/4$ and $n_2 = 1/2$, but such t values are far too large in the Fe-ludwigite ladder. But we see that the same regime can be reached in the A_I phase as well since, in this case, the effective hopping is zero in the c -direction which is equivalent to taking $t_c = 0$ (see Fig. 3) and the problem reduces to three sites. The I_a phase close to A_I with $\theta_1 = \theta_2$ could also give quite well the high temperature charge distribution as seen in Fig. 3 for $J_a S^2 / t_c \lesssim 0.2$. However, as can be seen in Fig. 3, an interesting point resulting from our analysis is the existence of the I_a structure with $\theta_1 \neq \theta_2$ as in Fig. 1-b. This produces a zig-zag bond alternation which, in turn, will give rise to a lattice instability of the same type. Due to the magnetic structure the two border sites of a rung have different electronic charges leading to the formation of a zig-zag charge ordering, $n_2 \approx n_3 \gg n_1$, similar to the one observed experimentally below T_c . Note that a phase of type $(\theta_1 = 0, \theta_2 = \pi/2)$, $\uparrow\uparrow \rightarrow$ on the rung, has been proposed at 10K⁸ in contrast with the antiferromagnetic ordering $\uparrow\downarrow\uparrow$ inside the triad obtained from earlier neutron experiments¹². Except asymptotically i.e. $J_a \rightarrow \infty$, we do not find phases with AF arrangement of the triads.

Finally we consider the effect of the lattice distortion of the rung with hopping $t_a(1 \pm \delta)$ alternating along the c -direction and we introduce an elastic energy term $\frac{1}{2}B\delta^2$ per rung. For an homogeneous magnetic state the model reduces to the simple Peierls model considered by Latgé and Continentino¹³ and is unlikely to reproduce the experimental behaviour for reasonable values of t even in the undimerized state as shown in Fig.4. As discussed above, the zig-zag I_a phase strongly favors the related rung distortion and, as expected, it occupies an important part of the phase diagram as shown in Fig.5 for a value $B/t_c = 6$. Here we do not consider the more complicated I_b phase appearing at lower J_c . Phase I_a shows two distinct regions, an undistorted one with $\theta_1 = \theta_2$ and

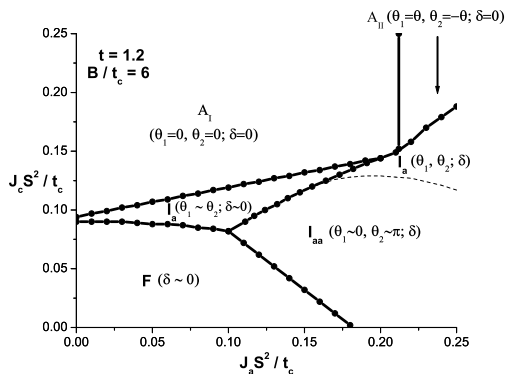


FIG. 5: $F-I_a$ phase diagram for the elastic parameter $B/t_c = 6$ as a function of $\frac{J_a S^2}{t_c}$ and $\frac{J_c S^2}{t_c}$. Note that A_I and A_{II} are particular cases of I_a . The distorted phase I_{aa} occurs below the dashed line.

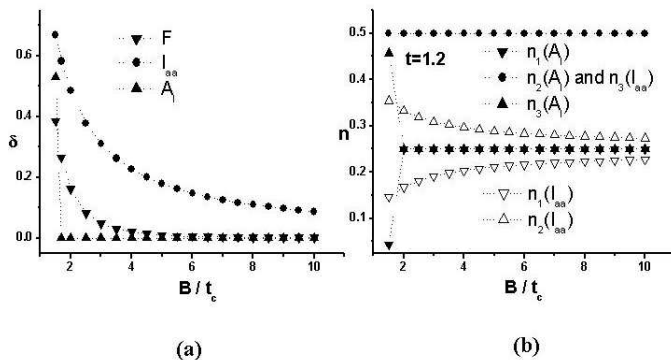


FIG. 6: (a) Lattice distortion of the rung among the F , A_I and I_{aa} phases as function of B/t_c . (b) The corresponding charges on the Fe sites in phases A_I and I_{aa} .

a wide distorted one. A phase I_{aa} with fully dimerized

hoppings ($\theta_1 = 0$, $\theta_2 = \pi$), one ferromagnetic and one antiferromagnetic bond in each rung, is now stabilized by the distortion (Fig.5, below the dashed line). The distortion δ for the F , A_I and I_{aa} phases is shown in Fig.6-a as function of B/t_c . The existence of hopping distortion $\delta \neq 0$ in A_I requires small values of the elastic term $B/t_c \lesssim \sqrt{2}t$. This is easily obtained from the total energy per rung E which reduces to $\frac{E}{t_c} = -t\sqrt{2(1+\delta^2)} + \frac{1}{2}\frac{B}{t_c}\delta^2$ in the 3-site problem. The I_{aa} phase presents the largest distortion among these phases, showing clearly the bond order related to the ferromagnetic character of the bonds. The corresponding charges on the Fe sites in phases A_I and I_{aa} are shown on Fig. 6-b. We see that the phase A_I represents better than others the experimental charges both above ($\delta = 0$) and below ($\delta \neq 0$) the structural transition T_c i.e n_2 remains constant equal to $1/2$, while $n_1 = n_3 = 1/4$ in the undistorted phase and n_3 approaches $1/2$ whereas n_1 decreases in the distorted phase. In the I_{aa} phase it is site-3 which has the largest electronic charge $n_3 = 0.5$ contrary to experimental estimate both above T_c and below for $74K < T < T_c$.

Our results are consistent with the existence of a A -type phase as proposed at $82K$ ⁸ but imply that it persists above T_c . On the other hand, the I -type structure proposed at $10K$ ⁸ should present charge ordering and lattice distortion, in contradiction with the recent Mössbauer results of Larrea et al.⁷. We have shown that simultaneous spin and charge ordering in qualitative agreement with the experimental behaviour for $T > 74K$ occurs from the competition between DE and SE interactions. The bonding is strongly reinforced by the ferromagnetic correlations, therefore this may induce a lattice instability as observed. Below $74K$, the experimental results^{7,8,11} are contradicting and further experiments are required to clarify the low temperature situation. Our approach has emphasized the importance of the magnetic structure and bring to light the interplay between spin ordering, charge ordering and lattice distortion.

We are grateful to J. Dumas, M. A. Continentino and P. Bordet for helpful discussions. E. V. acknowledge CONACYT for financial support.

¹ P. W. Anderson and H. Hasegawa, Phys. Rev. **100**, 675 (1955).
² P-G. de Gennes, Phys. Rev. **118**, 141 (1960).
³ D. J. Garcia, K. Hallberg, C. D. Batista, M. Avignon and B. Alascio, Phys. Rev. Lett. **85**, 3720 (2000).
⁴ H. Aliaga, B. Normand, K. Hallberg, M. Avignon and B. Alascio, Phys. Rev. B **64**, 024422 (2001).
⁵ M. Mir *et al.*, Phys. Rev. Lett. **87**, 147201 (2001).
⁶ J. Larrea J., D. R. Sanchez, F. J. Litterst, E. M. Baggio-Saitovitch, J. Phys.: Condens. Matter **13**, L949 (2001).
⁷ J. Larrea J., D. R. Sanchez, F. J. Litterst, E. M. Baggio-Saitovitch, J. C. Fernandes, R. B. Guimaraes and M. A. Continentino, Phys. Rev. B **70**, 174452 (2004).

⁸ P. Bordet *et al.*, (unpublished).
⁹ E. Carvajal, O. Navarro, R. Allub, M. Avignon and B. Alascio, Eur. Phys. J. B **48**, 179 (2005).
¹⁰ M.-H. Wangbo, H.-J. Koo, J. Dumas and M. A. Continentino, Inorg. Chem. **41**, 2193 (2002).
¹¹ A. P. Douvalis, A. Moukarika, T. Bakas, G. Kallias and V. Papaefthymiou, J. Phys.: Condens. Matter **14**, 3302 (2002).
¹² J. P. Attfield, J. F. Clarke and D. A. Perkins, Physica B **180-181**, 581 (1992).
¹³ A. Latgé and M. A. Continentino, Phys. Rev. B **66**, 094113 (2002).